

**DUAL KEEL SPACE STATION CONTROL/STRUCTURES
INTERACTION STUDY**

by

John W. Young
Spacecraft Control Branch

Frederick J. Lallman
Analytical Methods Branch

and

Paul A. Cooper
Structural Concepts Branch
NASA Langley Research Center
Hampton, VA 23665

ABSTRACT

A study was made to determine the influence of truss bay size on the performance of the space station control system. The objective was to determine if any control problems existed during reboost and to assess the level of potential control/structures interactions during operation of the control moment gyros used for vertical stabilization. The models analyzed were detailed finite-element representations of the 5-meter and 9-foot growth versions of the 300 KW dual keel station.

Results are presented comparing the performance of the reboost control system for both versions of the space station. Standards for comparison include flexible effects at the attitude control sensor locations and flexible contributions to pointing error at the solar collectors. Bode analysis results are presented for the attitude control system and control, structural, and damping sensitivities are examined.

PRECEDING PAGE BLANK NOT FILMED

The purpose and objectives of the study are presented in figure 1. Details of the space station models and the control systems studies are given in references 1 and 2.

PURPOSE

To determine the influence of truss bay size (5-meter vs. 9-foot) on the performance of the space station control systems

OBJECTIVES

- To assess the level of potential control/structures interactions during operation of the control moment gyros used for vertical stabilization
- To investigate possible control problems during operation of the Reaction Control System Jets used for orbit reboost

Figure 1

DUAL KEEL SPACE STATION

The 5-meter and 9-foot versions of the dual keel space station studied in the present paper had approximately the same dimensions and mass properties with the only difference being the truss bay size. The 5-meter station is shown in figure 2 to illustrate several points of interest in the control study. The control sensors and control moment gyros which constitute the Attitude Control Assembly (ACA) are co-located at the origin of the coordinate system shown in figure 2. The ACA package is located about 10 feet above the center of gravity of the station. The four reaction control system (RCS) thrusters shown are used in the reboost control system with each thruster producing a 75-pound force along the orbit plane (x-axis) of the station. The solar dynamic units are explained in a following figure. They are of interest in the reboost analysis since they must be oriented toward the solar vector for efficient operation as power generators.

ATTITUDE CONTROL SYSTEM STUDY

The attitude control system is designed to regulate the orientation of the space station to keep the longitudinal axis (z-axis) aligned with the gravity vector. The control system consists of y-axis pitch and pitch rate sensors, control moment gyros (CMG's), and electronics to cause corrective moments to be applied to the station whenever it deviates from the commanded attitude. The attitude control system study is outlined in figure 3. Control system performance indicators are listed in the figure.

ATTITUDE CONTROL SYSTEM STUDY

- Control System stability investigated using frequency response (Bode) Analysis

Control Laws:

- 1- Angular error and rate feedback (PD)
- 2- PD + 1st order lag compensation

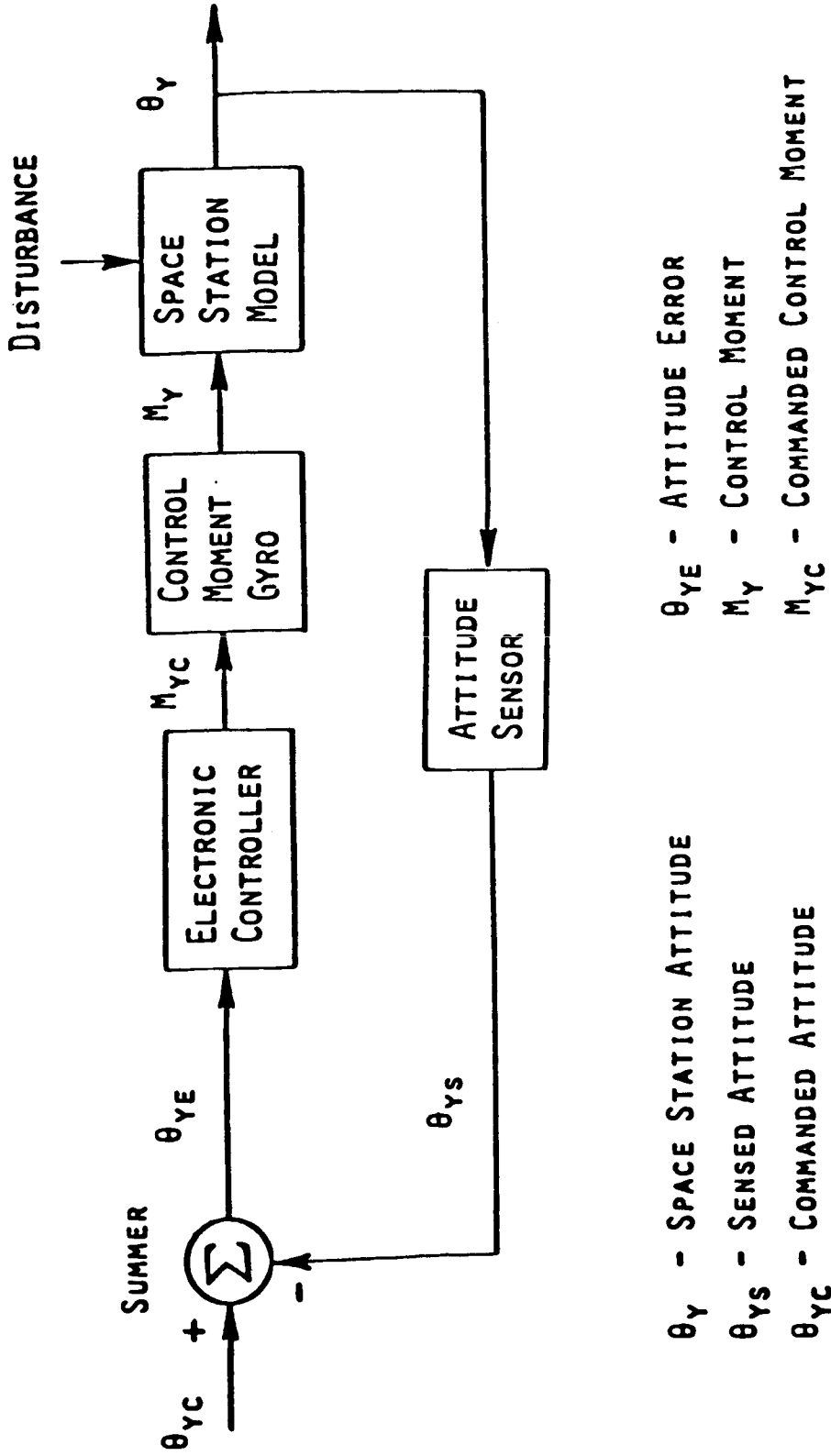
- Control System Performance Indicators

- 1- Gain margin for structural modes
- 2- Structural damping required for specified gain margin
- 3- Modal frequency change for structural instability
- 4- Control bandwidth

BLOCK DIAGRAM OF ATTITUDE CONTROL SYSTEM

A block diagram of the y-axis control system used in the study is shown in figure 4. The attitude angle (and its rate of change) responds to moments applied to the station by the CMG's and external and internal disturbances. The effect of structural vibrations is included in this angle. The electronic controller mechanized a control law to produce a commanded control moment based on the error signal. The closed loop bandwidth and damping ratio of the system was specified to be .01 Hz. and .275 respectively.

BLOCK DIAGRAM OF ATTITUDE CONTROL SYSTEM



θ_Y - SPACE STATION ATTITUDE
 θ_{YS} - SENSED ATTITUDE
 θ_{YC} - COMMANDED ATTITUDE

θ_{YE} - ATTITUDE ERROR
 M_Y - CONTROL MOMENT
 M_{YC} - COMMANDED CONTROL MOMENT

Figure 4

FREQUENCY RESPONSE, PD CONTROLLER

Frequency response plots for loop gain using a PD controller are given in figure 5. The PD controller is the simplest that can stabilize the rigid-body dynamics while meeting the bandwidth requirement. The low frequency portions of the plots reflect the rigid-body dynamics and are nearly identical since the moments of inertia of the two station models are approximately the same. The higher frequency portions of figure 5 show the effect of including the structural dynamics in the station models (50 structural modes were included). The major difference in the two models was that the structural mode frequencies of the 5-meter station were approximately twice those of the 9-foot configuration because of its greater stiffness. The frequency response plots of figure 5 indicate unstable gain margins for both station models with higher resonant peaks occurring with the 9-foot model.

FREQUENCY RESPONSE, PD CONTROLLER

$$\text{Control Law: } \frac{M_y}{\theta_{ye}}(s) = K's + K$$

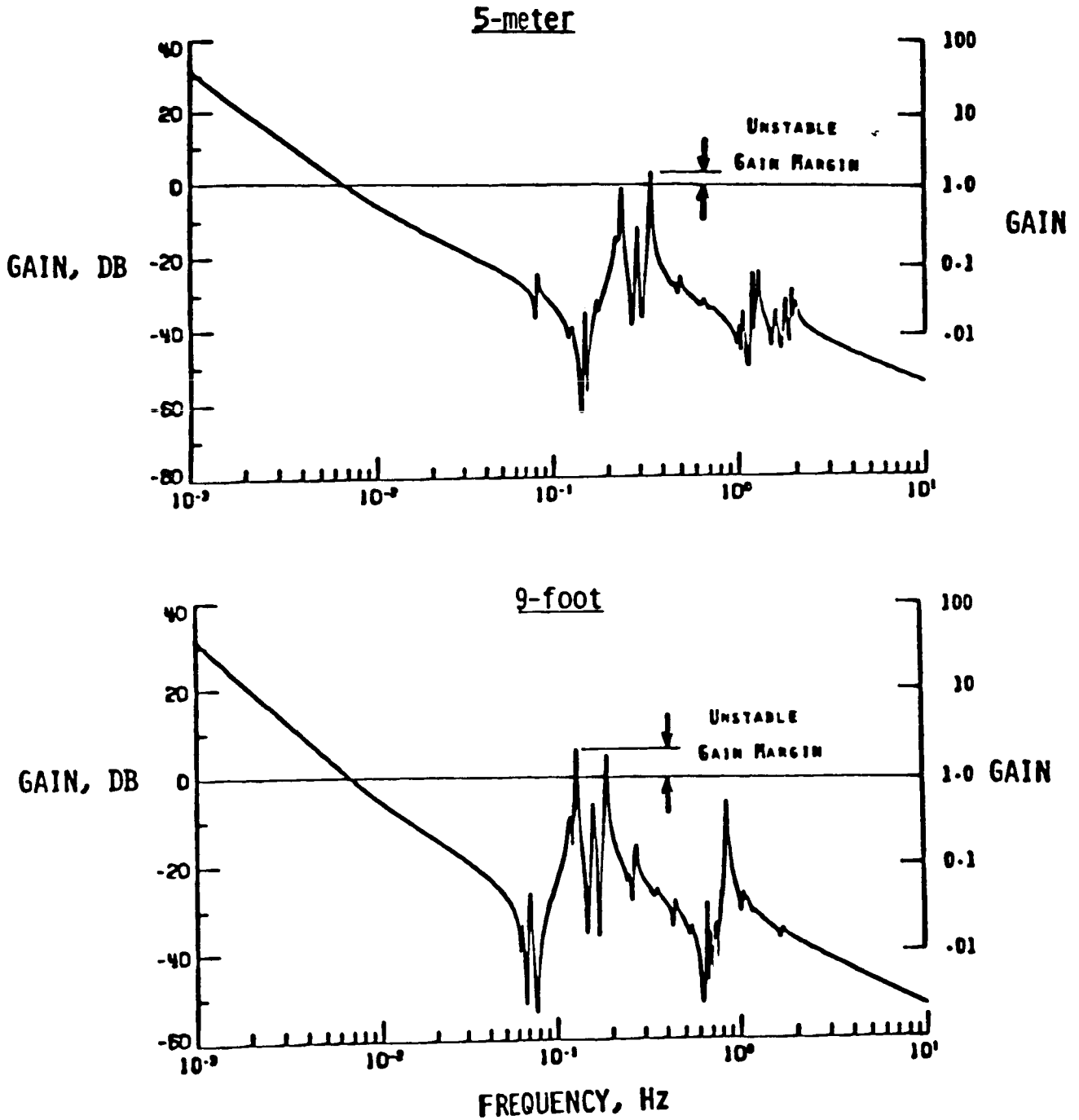


Figure 5

FREQUENCY RESPONSE, COMPENSATED PD CONTROLLER

Since the PD control law resulted in unstable structural modes, a second control law was designed to correct the problem. The object of the redesign was to reduce the magnitude of the frequency response for the higher frequency range while maintaining the rigid-body bandwidth and damping ratio. This was accomplished by adding a first-order lag to the control law and adjusting the proportional and differential gains to form a compensated PD controller. Frequency response plots for loop gain using the compensated PD controller are given in figure 6. The addition of compensation reduces the higher frequency portions of the gain plots and results in stable gain margins for both station models.

FREQUENCY RESPONSE, COMPENSATED PD CONTROLLER

$$\text{Control Law: } \frac{M_y}{\theta_{ye}} (s) = \frac{K's + K}{s/p + 1}$$

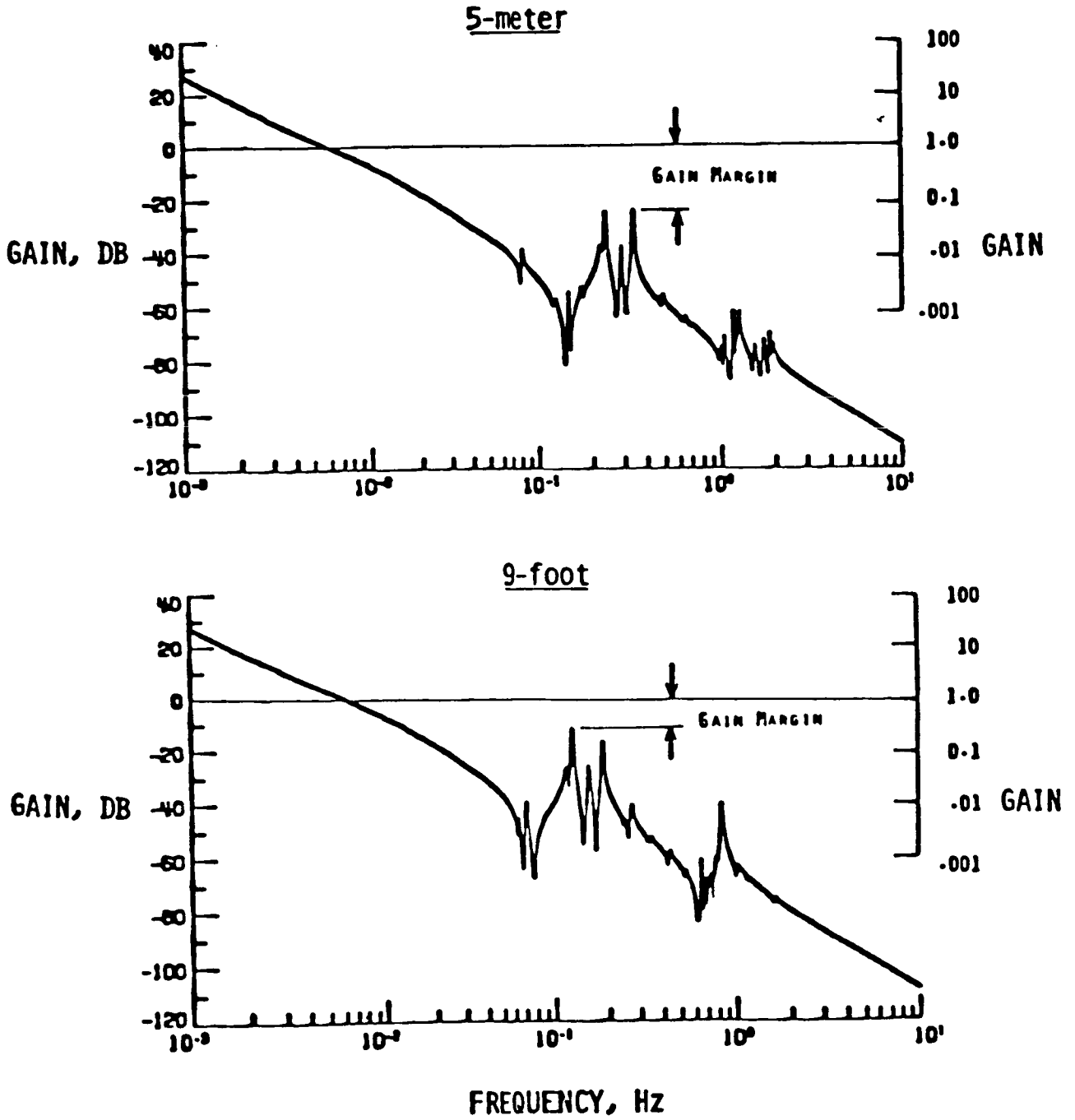


Figure 6

SPACE STATION BODE ANALYSIS RESULTS

The results of the attitude control system study using the compensated PD controller are given in figure 7. Gain margin comparisons (Fig. 6) show a 12 DB advantage for the 5-meter station. Estimates of the structural damping required to meet a hypothetical gain margin specification of 20 DB show that the 5-meter station required about 4.4 times less damping than the 9-foot model. The 5-meter station was found to be more tolerant to possible modal frequency changes and to have twice the bandwidth of the 9-foot station for a gain margin specification of 20 DB.

SPACE STATION BODE ANALYSIS RESULTS*

	<u>S</u> MEIER	<u>9</u> FOOI	COMMENTS
GAIN MARGIN	23 DB	11 DB	12 DB ADVANTAGE FOR 5-METER
REQUIRED STRUCTURAL DAMPING FOR 20 DB MARGIN	0.34%	1.5%	5-METER REQUIRES 4-5 TIMES LESS STRUCTURAL DAMPING
MODAL FREQUENCY CHANGE FOR STRUCTURAL INSTABILITY	-75%	-47%	5-METER IS MORE TOLERANT OF MODAL FREQUENCY CHANGES
MAXIMUM BANDWIDTH FOR 20 DB MARGIN	.012 Hz	.0060 Hz	5-METER ATTITUDE CONTROL IS TWICE AS RESPONSIVE

*PD CONTROLLER WITH 1ST ORDER COMPENSATION

Figure 7

REBOOST CONTROL SYSTEM STUDY

The reboost control system study performed is outlined in figure 8. Control system performance indicators are listed in the figure.

REBOOST CONTROL SYSTEM STUDY

- Control System performance comparisons between the 5-meter and 9-foot configurations were made using time history response calculations

Control Law:

Nonlinear switching logic for RCS jets based on sensed pitch and pitch rate

- Control System Performance Indicators
 - 1- Flexible interference in sensor outputs
 - 2- Structural vibrations at the solar collectors

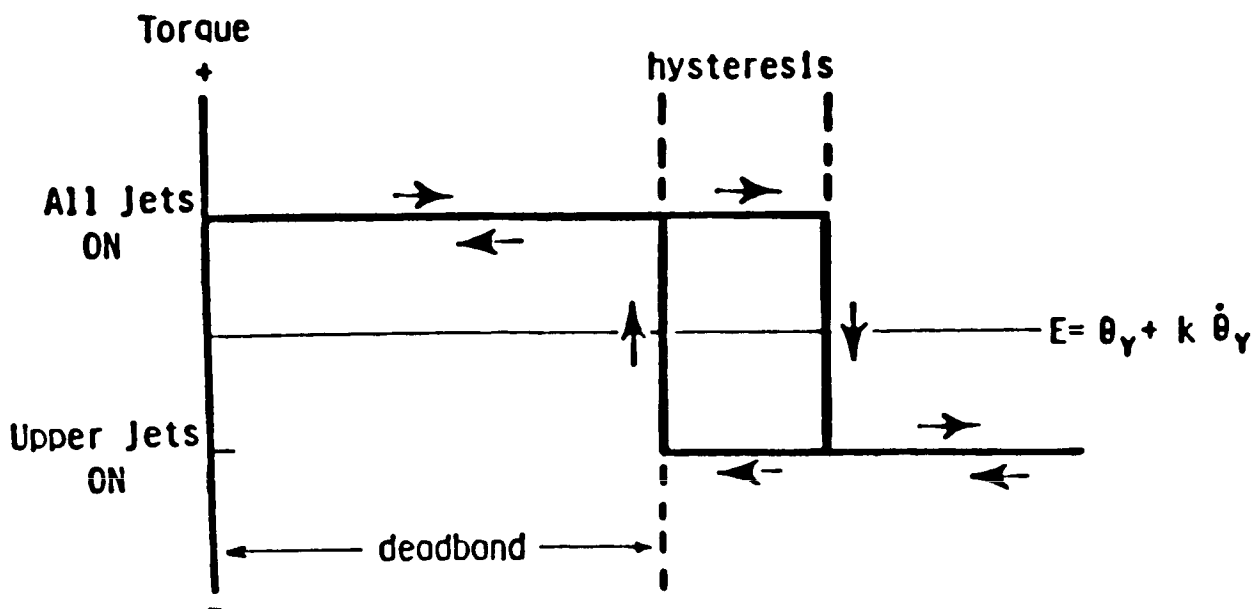
Figure 8

REBOOST CONTROL LOGIC

The Space Station must be periodically reboosted to maintain a desired orbit. The maneuver is performed using four 75-pound, constant thrust jets located as shown on figure 2 with two jets above and two below the station center of gravity. The purpose of the reboost control system is to maintain attitude control during the maneuver. The system operates either with all jets on or using only the upper jets. With all jets on, a torque is generated about the y-axis of the station causing it to rotate away from the local vertical. The station attitude is kept within desired limits by off-modulation of the lower-keel jets. The control logic which governs the firing of the lower jets is given in figure 9. The logic results in a near periodic firing of the RCS jets as shown in the control history given on figure 9. The 1-degree deadband results in the space station oscillating about a 1-degree offset from the local vertical.

REBOOST CONTROL SWITCHING CURVE FOR RCS JETS

(Deadband = 1° , Hysteresis = $.05^\circ$, $K = 1$ sec)



TYPICAL CONTROL HISTORY

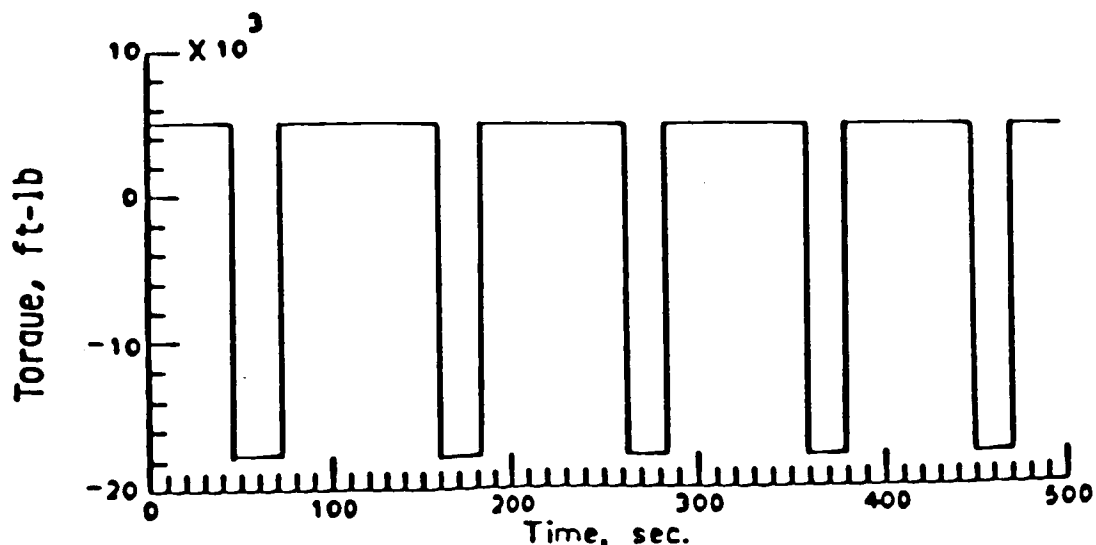


Figure 9

FLEXIBLE CONTRIBUTION TO ERROR SIGNAL DURING REBOOST MANEUVER

The error signal (E) used to control the RCS jet firing was an unfiltered pitch and pitch rate signal as measured at the ACA package location (Fig. 2). Since this signal contains both the rigid body and local flexible response, it is of interest to examine the flexible interference in sensor outputs during a reboost maneuver. Comparisons of the flexible contribution to the error signal are given in figure 10 for the 5-meter and 9-foot stations. The $.03^\circ$ peak in flexible interference for the 9-foot model could be reason for concern since it represents 60 percent of the $.05^\circ$ hysteresis used in the switching logic. However, no adverse effects were noted when an unfiltered error signal was used in the reboost logic. Nevertheless, with flexible deviations such as those shown on figure 10, the potential exists for deterioration of the hysteresis switching loop, and, in actual practice the reboost control error signal should be filtered to reduce flexible interference at the sensors.

FLEXIBLE CONTRIBUTION TO ERROR SIGNAL DURING REBOOST MANEUVER

$$(E_{flex} = \Theta_{y flex} + K \dot{\Theta}_{y flex})$$

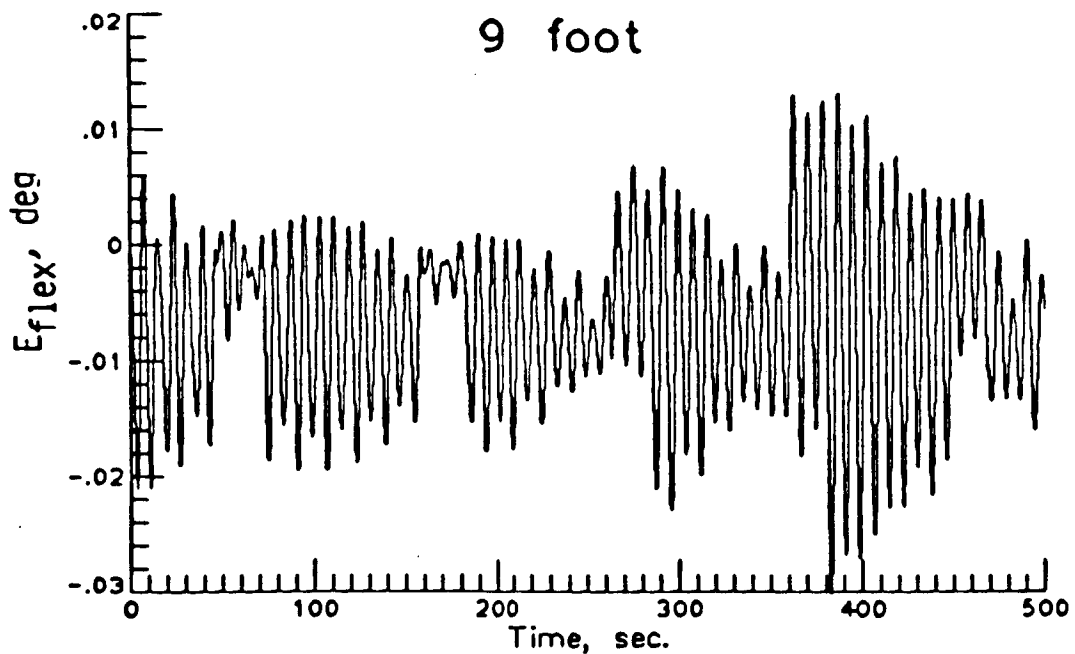
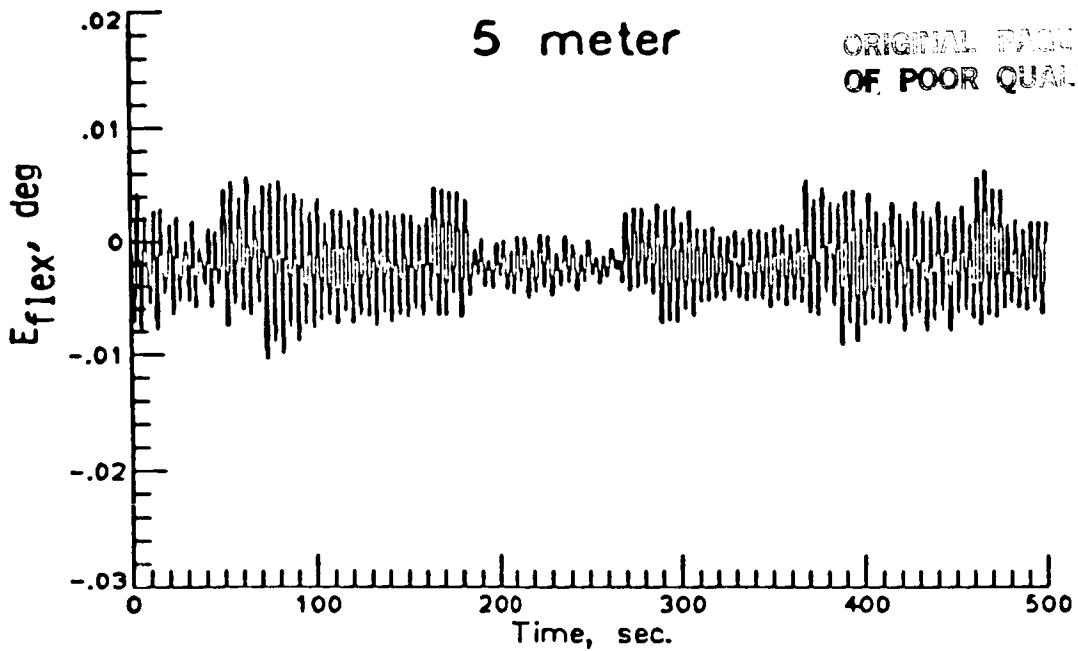


Figure 10

SOLAR DYNAMIC COLLECTORS

The station is powered by eight solar dynamic systems located as shown on figure 2. A typical solar dynamic collector is shown in figure 11. For maximum efficiency, the direction of the symmetric axis of each of the solar dynamic systems must be held to within $.1^\circ$ of the solar vector, even during an orbit reboost maneuver. This is done using controllers which command rotary joints located on the transverse truss and a rotary joint attached to the reflector symmetry axis. For the current study, these controllers are assumed inactive.

TYPICAL SOLAR DYNAMIC COLLECTOR UNIT

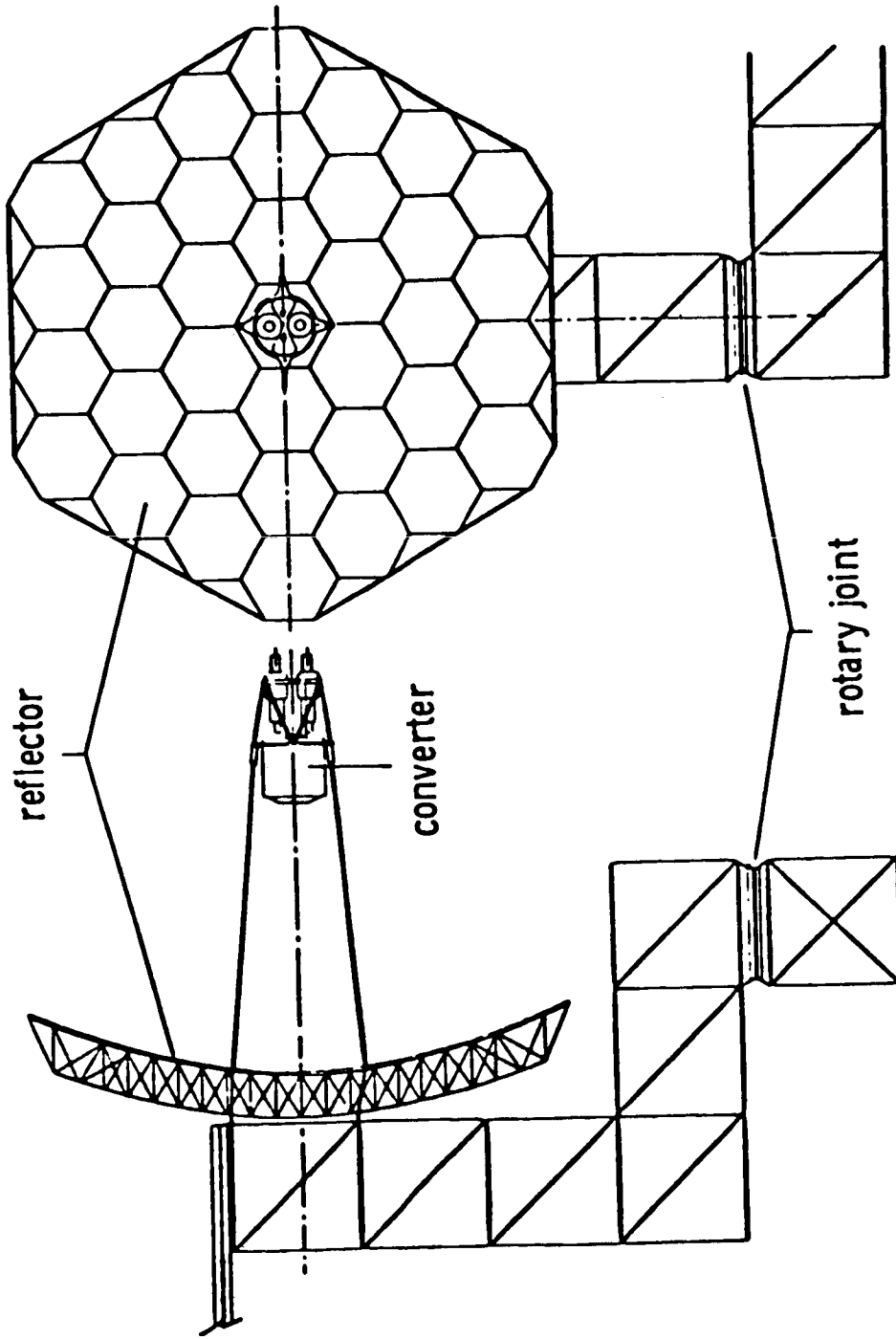


Figure 11

VARIATION OF SUN-LINE AT OUTER SOLAR COLLECTOR DURING REBOOST

Sun-line variations at the outer collector during reboost are shown on figure 12 for the 5-meter and 9-foot stations. The responses contain a low-frequency rigid-body oscillation with a superimposed, higher frequency oscillation caused by the flexible modes. Due to the 1-degree offset requirement during reboost, sun-line variations always exceed the $.1^\circ$ pointing requirement for the solar collectors. However, if the rigid-body pitch angle were known, it could be nulled using the previously discussed rotary joints. Note that the flexible variations shown in figure 12 are larger for the 9-foot station than for the 5-meter configuration.

VARIATION OF SUN LINE AT OUTER SOLAR COLLECTOR DURING REBOOST

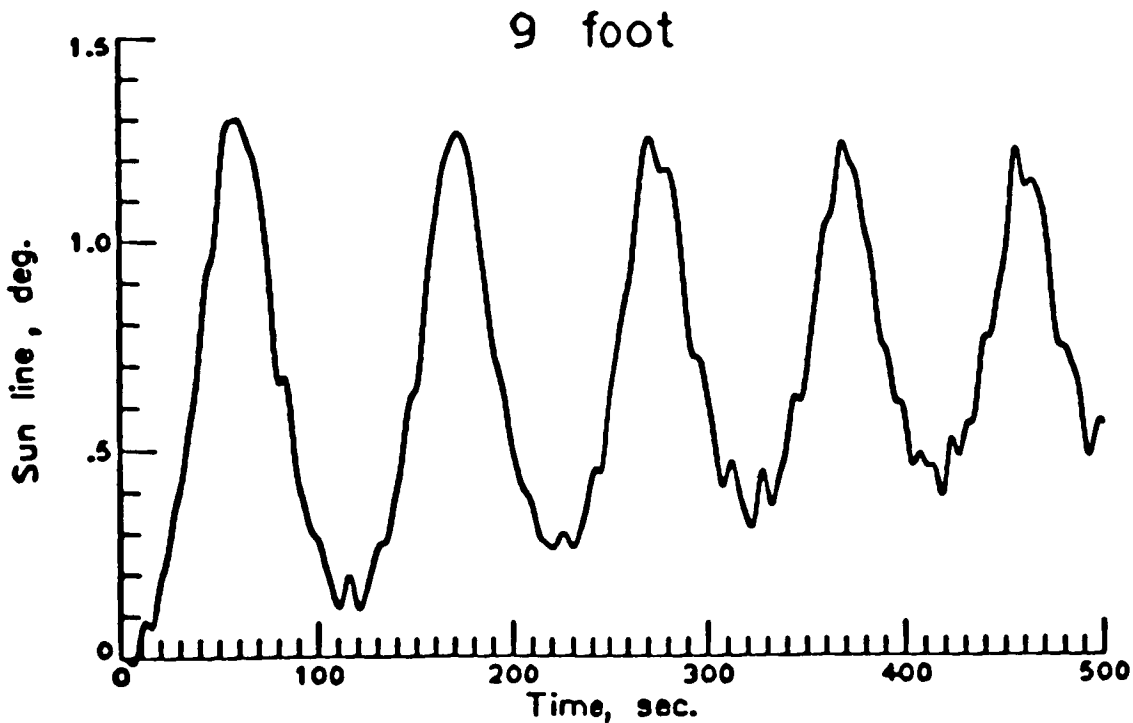
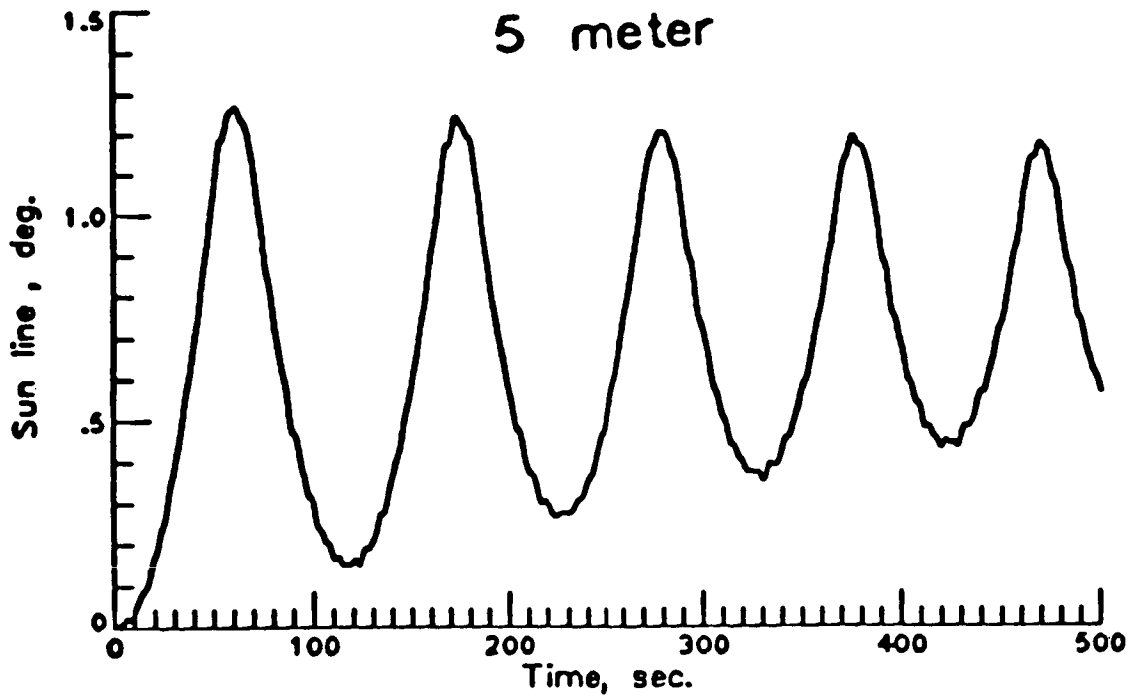


Figure 12

FLEXIBLE SUN-LINE EXCURSIONS DURING REBOOST

Flexible contributions to sun-line variations during reboost are given in figure 13 for the two station models. Shown is a continuous trace of the flexible sun-line at the outer solar collector during a reboost maneuver. While both flexible responses are within the $.1^\circ$ requirement, the 5-meter excursions are about one-fourth those for the 9-foot station.

SUN-LINE EXCURSIONS DURING REBOOST

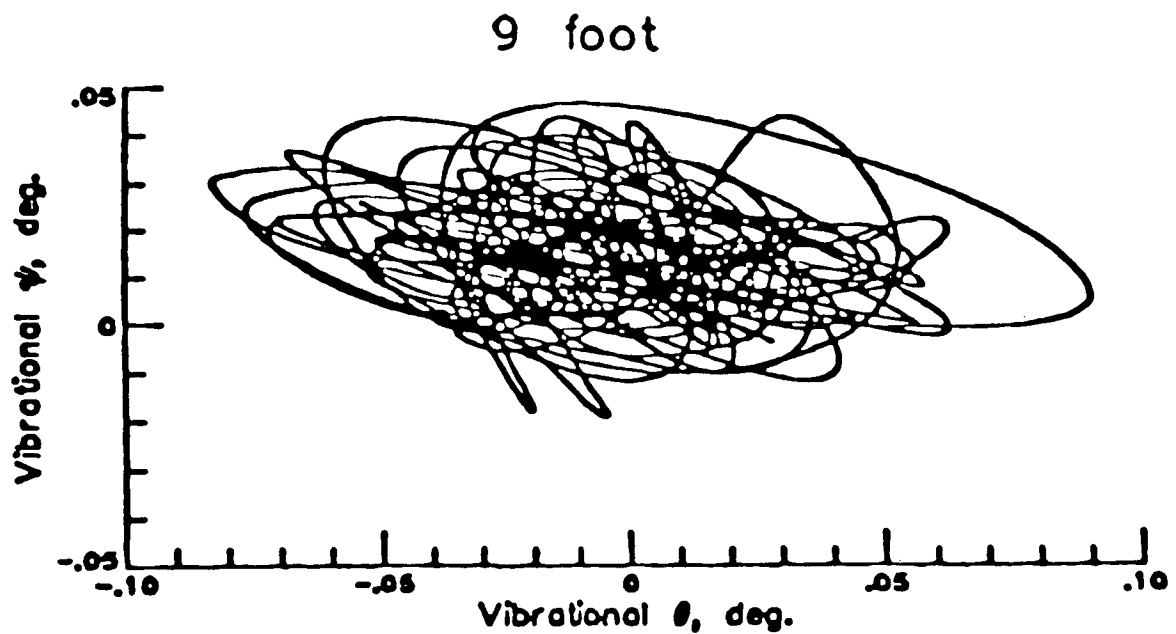
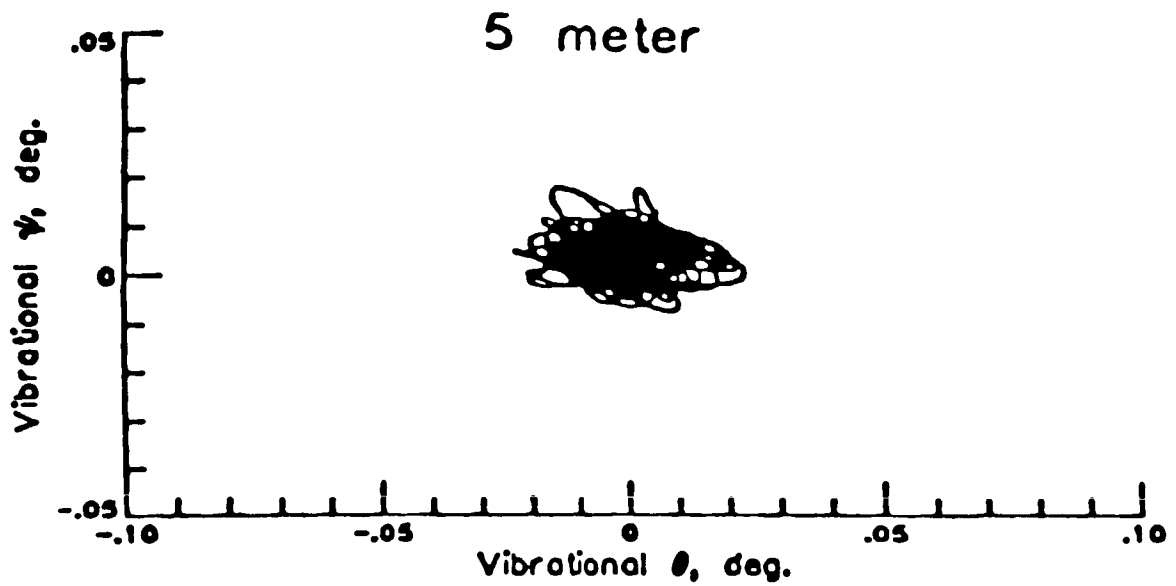


Figure 13

SUMMARY OF FLEXIBLE RESPONSE RESULTS FOR REBOOST MANEUVER

A summary of the results of the reboost control analysis are given in figure 14. The minimum structural frequency for the 5-meter station is double that for the 9-foot station. Since the reboost control frequencies are the same for both models, a greater separation between control and structural frequency exists for the 5-meter station. This is reflected in the lower flexible interference in the sensor outputs and the smaller collector transients shown in figure 14 for the 5-meter configuration.

SUMMARY OF FLEXIBLE RESPONSE RESULTS FOR REBOOST MANEUVER

	<u>5 meter</u>	<u>9 Foot</u>	<u>Comments</u>
Min. Structural Freq, Hz	.124	.062	5-meter freq double that for 9-foot
Reboost Control Freq, Hz	.014	.014	No difference
Peak Sensed E _{flex} , deg	.010	.030	5-meter interference 1/3 that for 9-foot
Peak Collector Transient, deg	.028	.095	5-meter peak sun-line transient about 1/4 that for 9-foot

Figure 14

REDESIGNED REBOOST MANEUVER

The previous reboost analysis assumed 75-pound thrust RCS jets, a 1-degree offset from the local vertical, and control logic hysteresis of $.05^\circ$. An additional study was made in which the control logic was redesigned such that total sun-line variations at the solar collectors would never exceed the $.1^\circ$ pointing requirement during the reboost maneuver. The redesign consisted of reducing the upper and lower RCS jets from 75 pounds to 12.5 pounds and 20 pounds respectively. This produced opposing torques of equal magnitude with all jets on or with only the upper jets active. The deadband in the control logic was set to zero and a hysteresis of $.00875^\circ$ was used. The resulting sun-line variation at the outer solar collector for the 5-meter station during reboost is shown in figure 15. Note that rigid-body plus flexible deviations remain within the $.1^\circ$ requirement throughout the maneuver.

VARIATION OF SUN LINE
AT OUTER SOLAR COLLECTOR
FOR REDESIGNED REBOOST MANEUVER

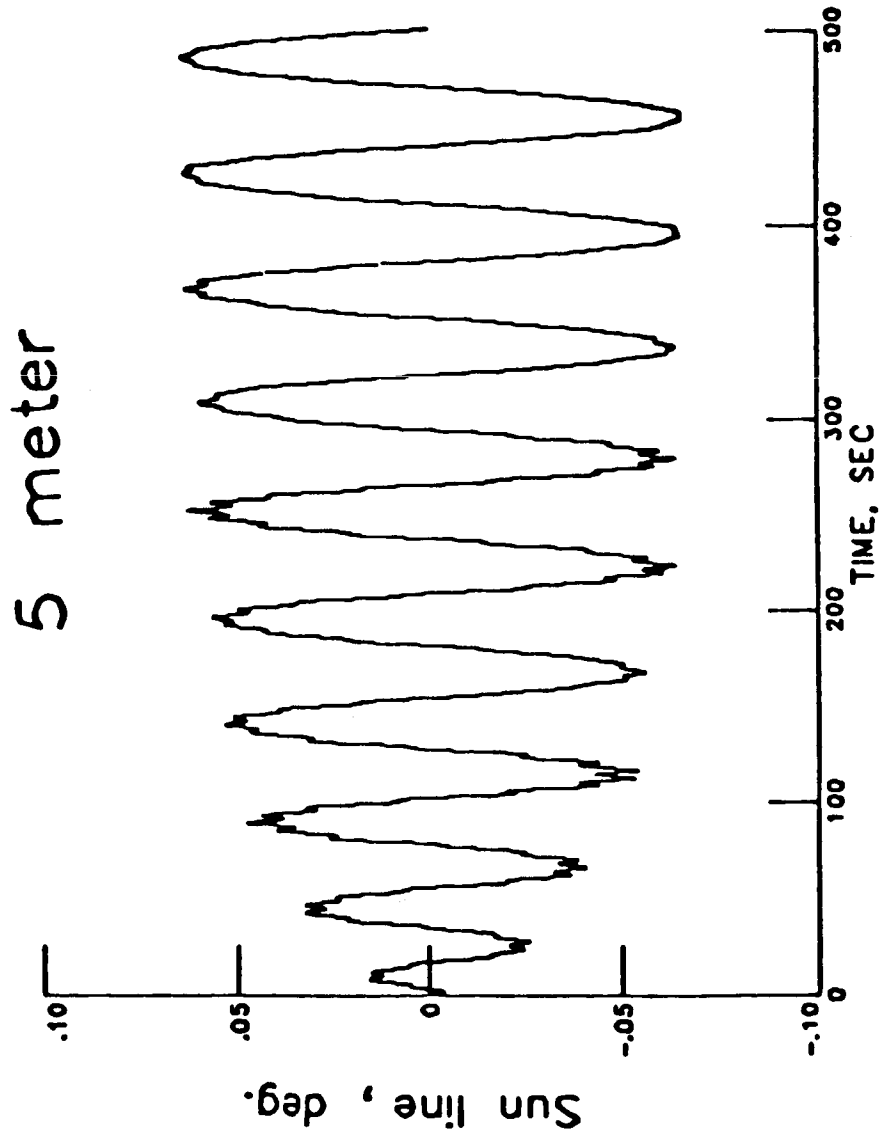


Figure 15

SUMMARY OF RESULTS

The reboost and attitude control study results are summarized in figure 16. All aspects of the control study indicated a preference for the 5-meter configuration.

SUMMARY OF RESULTS

REBOOST ANALYSIS

5-METER CONFIGURATION PREFERRED DUE TO:

- LOWER AMPLITUDE, HIGHER FREQUENCY INTERFERENCE
IN SENSED PITCH AND PITCH RATE
- SMALLER STRUCTURAL VIBRATIONS AT SOLAR
DYNAMIC COLLECTORS

ATTITUDE CONTROL (BODE) ANALYSIS

5-METER CONFIGURATION PREFERRED DUE TO:

- HIGHER GAIN MARGINS
- LOWER STRUCTURAL DAMPING REQUIREMENTS
- LOWER SENSITIVITY TO MODAL FREQUENCY VARIATIONS
- HIGHER BANDWIDTH

CONCLUSION

ALL ASPECTS OF THE CONTROL STUDY INDICATED A
PREFERENCE FOR THE 5-METER CONFIGURATION

Figure 16

REFERENCES

1. Dorsey, J. T.; Sutter, T. R.; Lake, M. S.; and Cooper, P. A.: Dynamic Characteristics of Two 300 KW Class Dual-Keel Space Station Concepts. NASA TM-87680, March 1986.
2. Young, J. W.; Lallman, F. J.; Cooper, P. A.; and Giesy, D. P.: Controls/Structures Interaction Study of Two 300 KW Dual-Keel Space Station Concepts. NASA TM-87679, May 1986.